Turkish Journal of Engineering
https://dergipark.org.tr/en/pub/tuje
e-ISSN 2587-1366

Investigation of the effect of additives on the microstructure of clay

Atila Demiröz [1], **Onur Saran** [*2]

[1] *Konya Technical University, Department of Civil Engineering, Türkiye, ademiroz@ktun.edu.tr*
[2] *Van Yüzüncü Yıl University, Department of Civil Engineering, Türkiye, onursaran@yyu.edu.tr*

Cite this study: Demiröz, A., & Saran, O. (2024). Investigation of the effect of additives on the microstructure of clay. Turkish Journal of Engineering, 8 (3), 563-571

https://doi.org/10.31127/tuje.1439113

Keywords
Soil stabilization
Basalt fiber
XRD
SEM

Research Article

Received: 18.02.2024
Revised: 19.03.2024
Accepted: 25.03.2024
Published: 15.07.2024

Abstract

In civil engineering, some soils cause many problems in terms of geotechnical engineering. Especially high plasticity clayey soils cause serious problems in road, airport, pavement and highway construction. Such soils can be stabilized using the chemical stabilization method. Additives such as lime, cement, fly ash and blast furnace slag are generally used in chemical stabilization. In addition, in recent years, there have been many studies on the use of natural and artificial fibers in ground stabilization. In this study, the effects of basalt fiber and mineral additives on the microstructure of clay soil were examined. Microstructures of pure and additively mixed clayey soil specimens were investigated for this purpose. X-ray diffraction (XRD) and scanning electron microscopy (SEM) analyses were performed on compacted soil specimens. In sum, it has been shown that the addition of lime, fly ash, and silica fume is effective in improving the compactivity properties. Pore sizes in SEM images vary depending on additive addition. SEM images showed that the soil particles adhered to the basalt fiber surface, which contributed to the force and friction between the soil particles and the basalt fiber.

1. Introduction

Expansive soils are frequently encountered in geotechnical engineering applications. In general, soils with low strength, high compressibility, and high volumetric changes cause a slew of problems. Before using clayey soils in roads, airports, sidewalks, and highways, they must be improved. Soil stabilization leads to a decrease in the soil's plasticity and swelling potential while increasing soil strength and workability [1-2]. Chemical or mechanical techniques can be used to achieve stabilization. In situations where mechanical stabilization is inadequate, chemical stabilization is utilized. Chemical stabilization involves adding various chemical additives to the soil to initiate reactions that enhance its strength, durability, and compression properties. Chemical stabilization is usually accomplished by incorporating additives into the soil, such as cement, asphalt, lime, and fly ash [3-5].

Stabilizations with cement and lime are widely used globally. Stabilized soils go through cementation and ion exchange reactions, which enhance the soil's chemical and mechanical characteristics. Previous studies have focused on the improved soils' geotechnical behavior [6-9].

Lime and cement are useful additives for fine-grained soils. When lime or cement additives are mixed with soil, cation exchange, flocculation and agglomeration, cementitious hydration, and pozzolanic reactions take place, which improve the clay's properties [10]. While cation exchange occurs in a short time, pozzolanic reactions take place over a longer period. When lime is added to the soil, pozzolanic reactions result in the formation of products such as hydrated calcium silicate (CS), hydrated calcium aluminate/silicate (CAS/CAH) [11-13]. Calcium silicate/alumina hydrate gels improve soil's mechanical properties by filling voids. A number of researchers have investigated the relationship between improved soil microstructure and geotechnical engineering behavior [14-16].

In the last few years, in addition to such additives, the number of studies involving fibers in ground stabilization has increased. One of these fibers is basalt fiber. Basalt fiber is obtained by melting basalt rock at high temperatures and then pulling it as fibers. Studies have shown that fibers have good properties and can interact with soil particles to increase overall strength when mixed with soil. In geotechnical engineering, the use of fiber reinforcement in soil stabilization enhances soil strength, prevents the formation of tensile cracks,

prevents swelling tendencies in expansive soils, improves hydraulic conductivity and liquefaction resistance, and reduces soil brittleness. Furthermore, basalt fiber, among other fibers, is an environmentally friendly and pollution-free high-tech fiber. The three-dimensional structure created among the fibers reduces soil deformations, forms a friction surface between the soil particles and the fibers, and improves the mechanical properties of the soil [17-21].

In this study, the effect of basalt fiber and mineral additives (lime, fly ash, and silica fume) on the microstructure of high plasticity clayey soil has been investigated. To investigate the effects of additives on soil composition, both X-ray diffraction (XRD) and scanning electron microscopy (SEM) were conducted on samples with and without additives.

2. Method

2.1. Soil properties

In the study, a high plasticity clay (CH) soil exhibiting swelling properties was used. The clayey soil used in the study was obtained from an area in Konya province, Selçuklu district, 2nd Organized Industrial Zone. About 5 tons of clayey soil were excavated from a depth of 6–7 m below the surface, put into a truck, and driven to the geotechnical laboratory at Konya Technical University. Sieve analysis, hydrometer test, Atterberg limits, and pycnometer test were conducted according to the relevant ASTM standard to determine the basic physical properties of the soil (Table 1).

Table 1. Physical properties of soil.

Liquid limit, ω_L (%)	105
Plastic limit, ω_p (%)	31
Plasticity index (I_P) (%)	74
Specific gravity	2.65
Maximum dry density, ρ_{kmax} (g/cm^3)	1.45
Optimum moisture content, w_{opt} (%)	28.5
Soil classification (USCS)	CH

2.2. Properties of additive materials

Lime (L): In the study, Erciyes TS EN 459-1 CL 80-S hydrated lime has been used.

Fly ash (FA): The experimental study used fly ash obtained from the Kütahya Seyitömer Thermal Power Plant. The obtained fly ash meets the ASTM C 618 standard, with a combined SiO_2+Al_2O_3+Fe_2O_3 content of 84.34% (S+A+F > 70%) and a CaO content of less than 10%, categorizing it as Class F (low-calcium) fly ash.

Silica fume (SF): The silica fume additive used in the study was obtained from Antalya Elektrometalurji A.Ş.

The compositions of the chemicals of the additives are shown in Table 2. The chemical analysis results of the additives have been obtained from the companies from which they have been supplied.

2.3. Basalt fiber (BF)

Basalt fibers have been supplied by Spinteks Textile Construction Industry and Trade Inc. (Denizli/Türkiye) (Figure 1). The fibers are 6, 12, 18, and 24 mm in length.

Table 2. Chemical composition of additives used in the study.

Chemical Composition	Silica Fume (SF) (%)	Fly ash (FA) (%)	Lime (L)
SiO_2	79.94	54.49	-
Al_2O_3	0.83	20.58	-
Fe_2O_3	0.41	9.27	-
CaO	2.53	4.26	≥80
MgO	7.68	4.48	≤5
K_2O	-	2.01	-
SO_3	-	0.52	≤2
C	1.22	-	-
S	0.923	-	-
CO_2	-	-	≤7
Free lime			≥65
Loss of ignition	2.96	3.01	

Figure 1. Basalt fibers.

Two different experimental design tables have been created using the Taguchi method for experimental studies. The Taguchi method is an experimental design method that tries to minimize the variability in the product and process by choosing the most appropriate combination of levels of controllable factors against the uncontrollable factors that create variability in the product and process. The Taguchi experimental design method involves a series of steps: Firstly, identifying the problem requiring improvement, then selecting and standardizing the variables affecting performance characteristics. Next, selecting an appropriate orthogonal array, assigning factors and interactions to columns, and choosing quality loss functions along with performance statistics. Following this, conducting experiments, recording results, analyzing data, and determining the optimal values for controllable variables. Within this method, measurement outcomes are transformed into Signal/Noise (S/N) ratios. These ratios represent the ratio of the desired actual value from the system to a factor not initially considered but influencing the test outcome. In this context, 'signal' is denoted by S, and 'noise' by N. Enhanced product quality is achieved through higher S/N ratios, achieved by maximizing signal and minimizing noise. Calculation methods for S/N ratios vary, with the most common being 'Larger is Better', 'Smaller is Better', and 'Nominal is Best' approaches [22].

3% lime was added to all designs containing basalt fiber-fly ash and basalt fiber-silica fume additives to increase pozzolanic interaction. The percentage of lime added to the soil may vary depending on its use to stabilize the soil or increase its workability. Small

amounts of lime are required to increase workability, while large percentages of lime are required to increase stability. Previous studies have shown that a minimum of 3% lime addition is required for the stabilization of high plasticity clay soil [23-24]. For this reason, the lime percentage was chosen as 3% in this experimental study. Additionally, additive contents were determined by taking into account the optimum additive percentages obtained in studies in the literature.

Unconfined compressive tests (UCS) were performed on samples prepared at optimum water content and maximum dry density values. Average unconfined compressive strengths (q_u) were obtained by performing experiments on three samples for each design. The test design table, compaction parameters and unconfined compressive strengths are given in Table 3 and Table 4.

Table 3. Taguchi L_{16} orthogonal experiment table (BF+SF) and unconfined compressive strength values

Design No	Parameters				$\rho_{k,max}$ (g/cm³)	w_{opt} (%)	q_u (kPa)
	A	B	C	D			
	BF Length (mm)	BF content (%)	Curing Time (days)	SF content (%)			
1	6	0	1	0	1.394	32.0	296.7
2	6	0.5	7	5	1.380	32.6	874.9
3	6	1	28	10	1.360	32.7	1299.9
4	6	1.5	56	15	1.336	33.7	1326.5
5	12	0	7	10	1.358	33.0	1081.4
6	12	0.5	1	15	1.333	33.5	593.6
7	12	1	56	0	1.386	31.9	961.3
8	12	1.5	28	5	1.367	32.7	1157
9	18	0	28	15	1.340	33.7	1181.6
10	18	0.5	56	10	1.351	33.0	1521.3
11	18	1	1	5	1.375	32.7	558.5
12	18	1.5	7	0	1.379	31.8	761.6
13	24	0	56	5	1.374	32.7	881.5
14	24	0.5	28	0	1.384	31.9	847.3
15	24	1	7	15	1.339	33.8	1282.4
16	24	1.5	1	10	1.352	32.9	565.4

Table 4. Taguchi L_{16} orthogonal experiment table (BF+FA) and unconfined compressive strength values

Design No	Parameters				$\rho_{k,max}$ (g/cm³)	w_{opt} (%)	q_u (kPa)
	A	B	C	D			
	BF Length (mm)	BF content (%)	Curing Time (days)	FA content (%)			
1	6	0	1	0	1.394	32.0	296.7
2	6	0.5	7	5	1.349	33.0	813.7
3	6	1	28	10	1.340	33.5	1205.1
4	6	1.5	56	15	1.314	34.4	1194.0
5	12	0	7	10	1.338	33.7	1005.7
6	12	0.5	1	15	1.311	34.3	529.7
7	12	1	56	0	1.386	31.9	961.3
8	12	1.5	28	5	1.356	33.1	1064.4
9	18	0	28	15	1.320	34.3	1119.7
10	18	0.5	56	10	1.332	33.4	1354.0
11	18	1	1	5	1.350	33.0	513.8
12	18	1.5	7	0	1.379	31.8	761.6
13	24	0	56	5	1.356	33.2	819.8
14	24	0.5	28	0	1.384	31.9	847.3
15	24	1	7	15	1.311	34.4	1179.8
16	24	1.5	1	10	1.327	33.6	531.1

XRD and SEM analyses were carried out on the pure soil sample, Design 10 samples with the highest strengths, and Design 7 and Design 9 samples with lower strengths to determine the effect of changes in fly ash and silica fume content on microscopic structure. XRD and SEM analyzes were carried out on selected designs in order to observe and interpret the microstructures of pure and added soil samples prepared by compaction at optimum water content and maximum dry density (Figure 2). Additionally, the microstructures of soil-lime-basalt fiber and fly ash/silica fume mixtures were investigated in correlation with UCS results.

3. Results and discussion

The crystal phases determined by X-ray diffraction (XRD) analysis for different mixtures and the pure soil sample are given in Figure 3-8. The XRD analysis results revealed the formation of Tobermorite (calcium silicate/aluminate hydrate (C-S-H)) mineral due to the pozzolanic reaction of lime, fly ash, and silica fume additives. The calcium silicate hydrate peak formed at 29.7°, and according to the analysis results, the presence of quartz (SiO_2) has been observed in the samples. The density of quartz has decreased due to the pozzolanic

reaction of the additives. Tiwari et al. [25] reported that this situation is due to the consumption of quartz minerals during the C-S-H formation.

The density of the calcium silica/alumina hydrate mineral was found to be higher in the designs with the highest strength (design no 10). This indicates that the formation of hydrated gel during curing occurs at higher concentrations with longer curing times and the use of optimal strength parameter levels. XRD analysis results of Design-7 (3% lime and basalt fiber-added sample) and Design-10 (3% lime, 10% fly ash/silica fume and basalt fiber-added samples) cured for 56 days showed that the intensity of C-S-H mineral increased by adding fly ash or silica fume to the lime.

Figure 2. Performing XRD and SEM analyses.

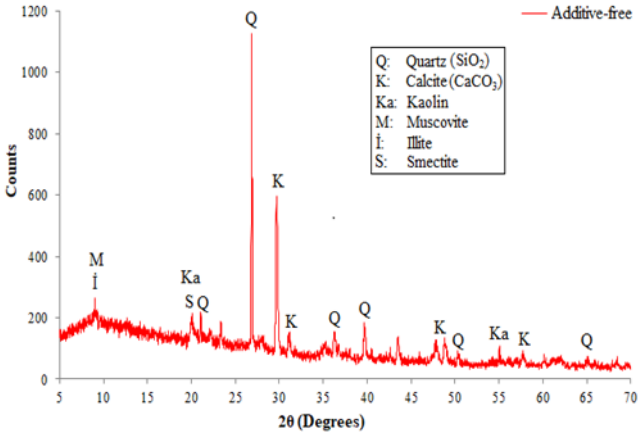

Figure 3. XRD analysis results of pure soil.

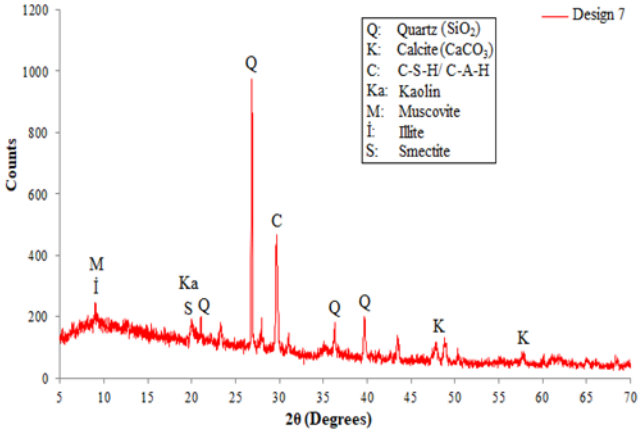

Figure 4. XRD analysis results of Design 7.

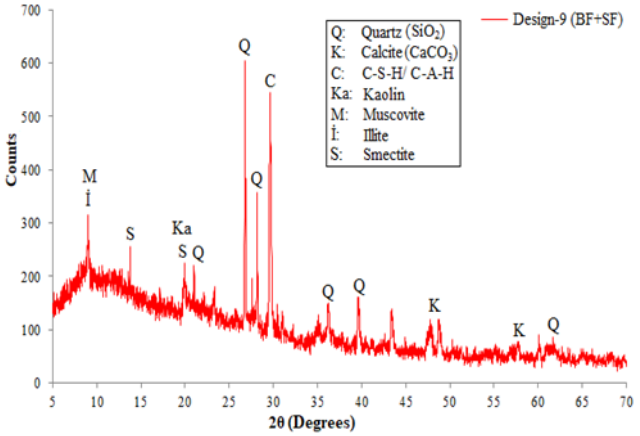

Figure 5. XRD analysis results of Design 9 (BF+SF).

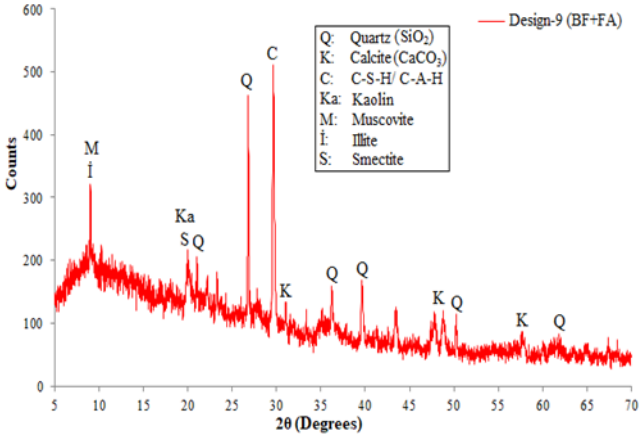

Figure 6. XRD analysis results of Design 9 (BF+FA).

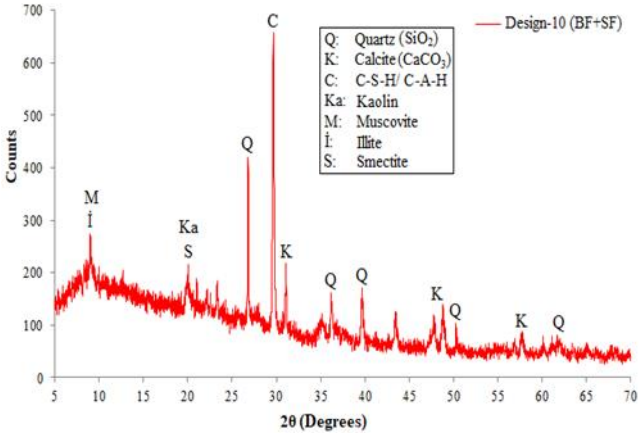

Figure 7. XRD analysis results of Design 10 (BF+SF).

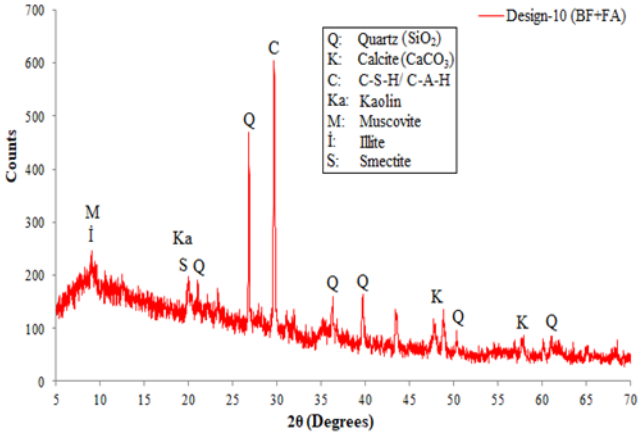

Figure 8. XRD analysis results of Design 10 (BF+FA).

SEM images obtained from selected design samples are given in Figure 9-14.

When the SEM images of the pure soil sample were examined, they showed a more dispersed and void

structure (Figure 9). When adding lime to the soil, the lime comes together to form a more cohesive mass due to pozzolanic and cation exchange reactions. The clayey soil exhibited a more granular structure with 3% lime contribution (Figure 10).

In addition to the lime additive, the addition of fly ash and silica fume led the particles to reorganize and increase structural integrity (Figure 11-13). This finding can be explained by the increased silica concentration due to the addition of both fly ash and silica fume and the rapid agglomeration of particles, leading to an increase in particle size. The addition of fly ash/silica fume developed the arrangement of clay particles to change from dispersed to lumped, resulting in the formation of some new cement-like compounds. The surfaces of the particles are generally coated with hydration gels and the soil pores are largely filled. This situation is caused by the beneficial effects of lime + fly ash or lime + silica fume additives on the formation of additional cementitious phase.

This improvement in soil properties is attributable to the quick development of the silicate gel and the increased synthesis of a new cementitious compound composed of calcium ions (Ca^{+2}) from lime and silicon dioxide (SiO_2) from silica fume [24, 26]. This can quickly fill soil voids and firmly interlock clay particles. As a result of the increased additive content, the soil's geotechnical properties improved. Increased lime and silica fume or lime and fly ash mixtures produced higher strength values than mixtures with 3% lime additives, owing to larger particle size and aggregation dimension.

SEM images show that soil particles adhere to the surface of basalt fiber, contributing to the force and friction between soil particles and basalt fiber (Figure 14). Tang et al. [27] reported that the contact area of fibers and surface roughness have significant effects on the micro-mechanical properties of the fiber-clay interface and that soil particles adhering to the fiber surface improve the interface bond.

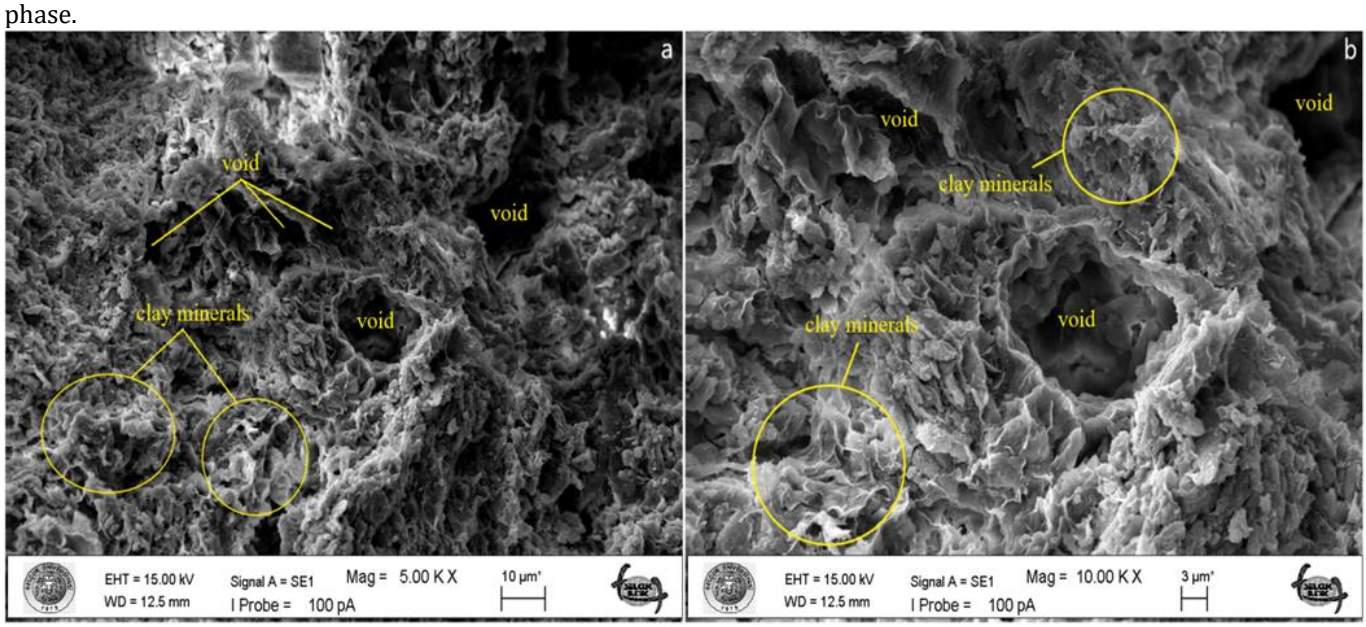

Figure 9. SEM image of clay soil with no additives; a. 5000X magnification b. 10000X magnification.

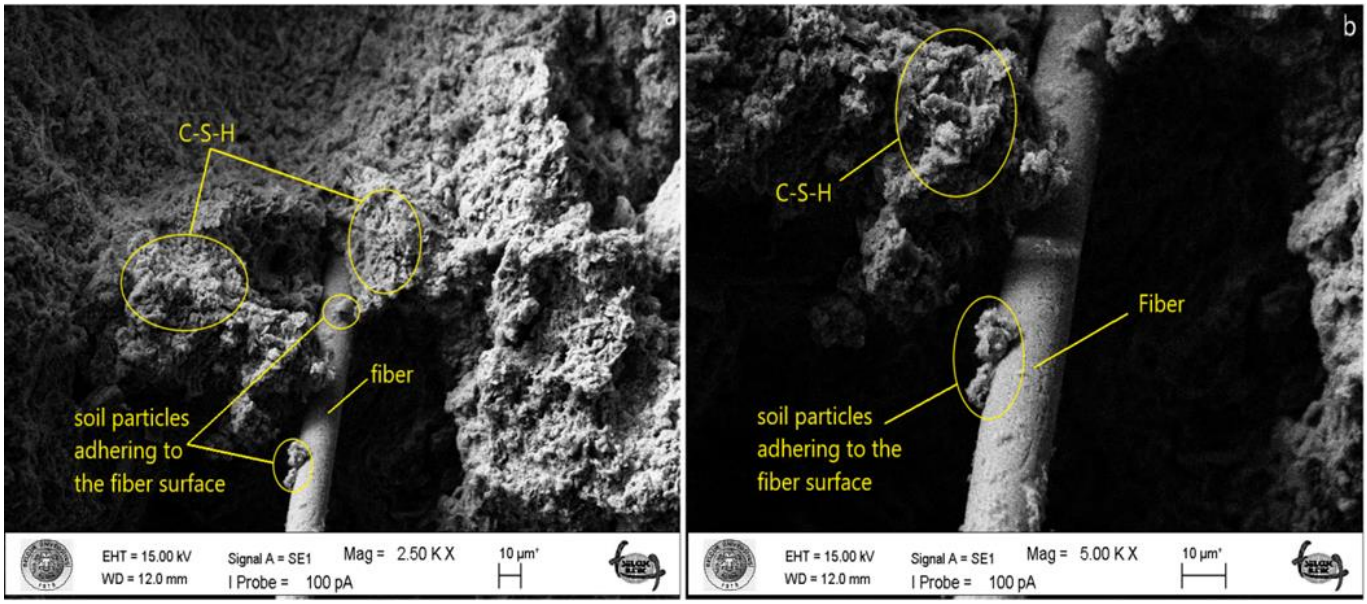

Figure 10. SEM image of design 7 (3%L+1%BF additives) a. 2500X magnification; b. 5000X magnification.

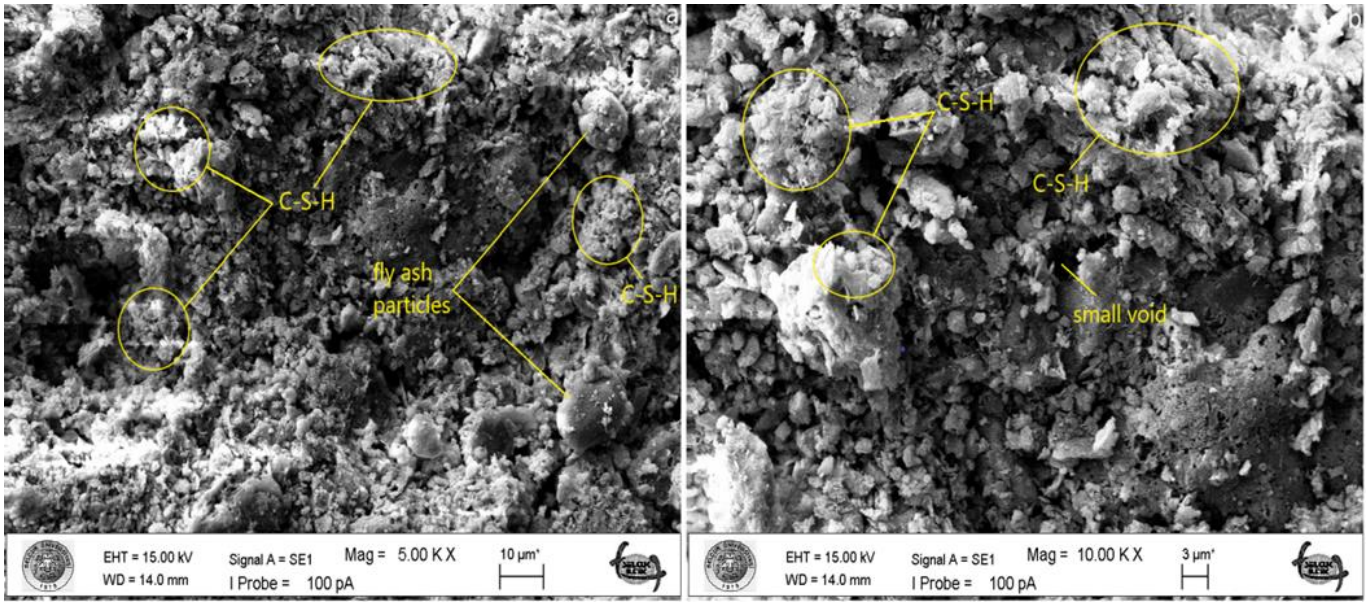

Figure 11. SEM image of design 9 (%3L+%15FA additives) a. 2500X magnification; b. 5000X magnification.

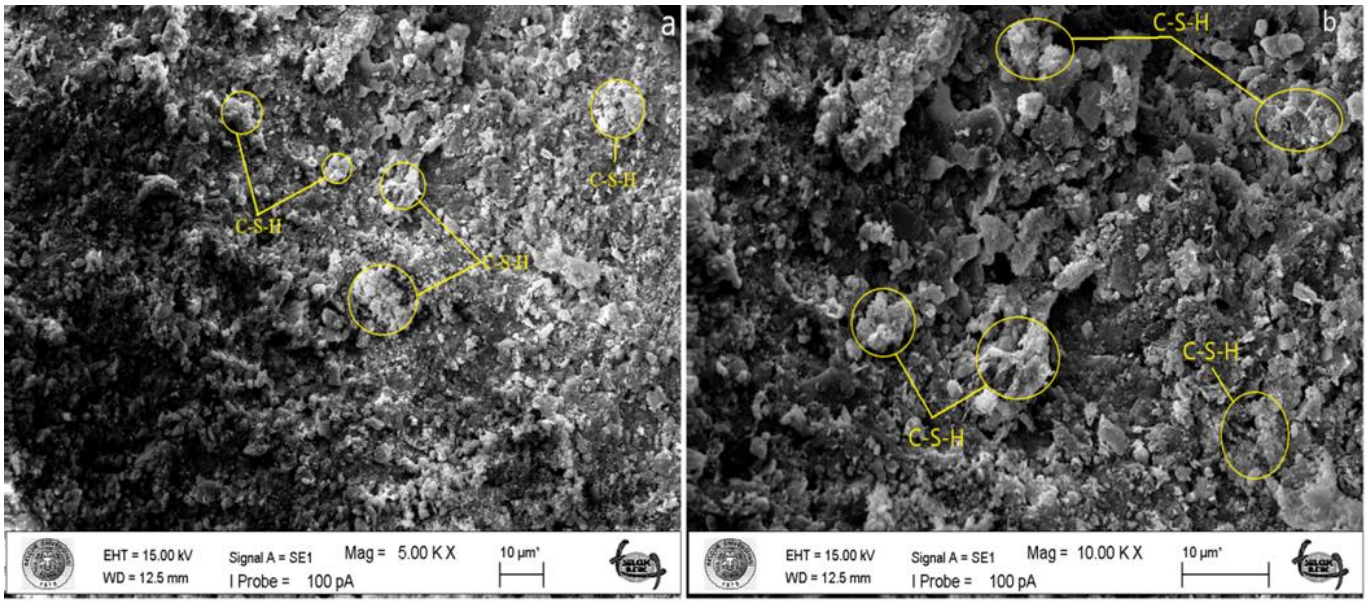

Figure 12. SEM image of design 9 (%3L+%15FA additives) a. 2500X magnification; b. 5000X magnification.

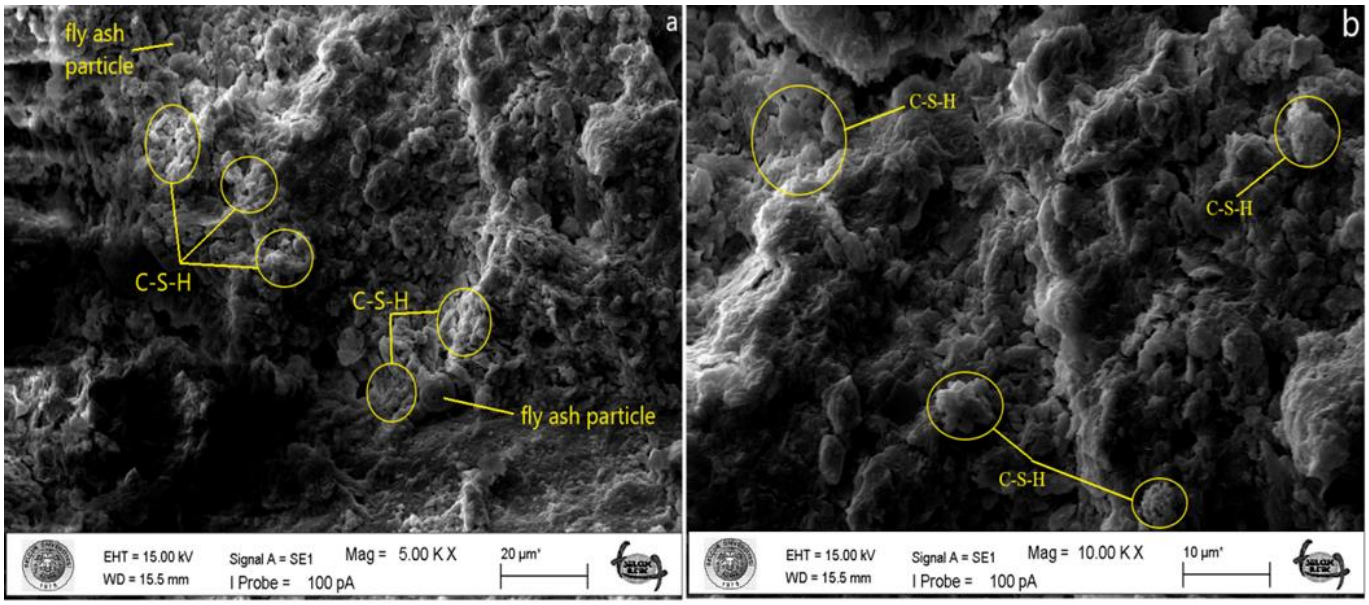

Figure 13. SEM image of design 9 (%3L+%15FA additives) a. 2500X magnification; b. 5000X magnification.

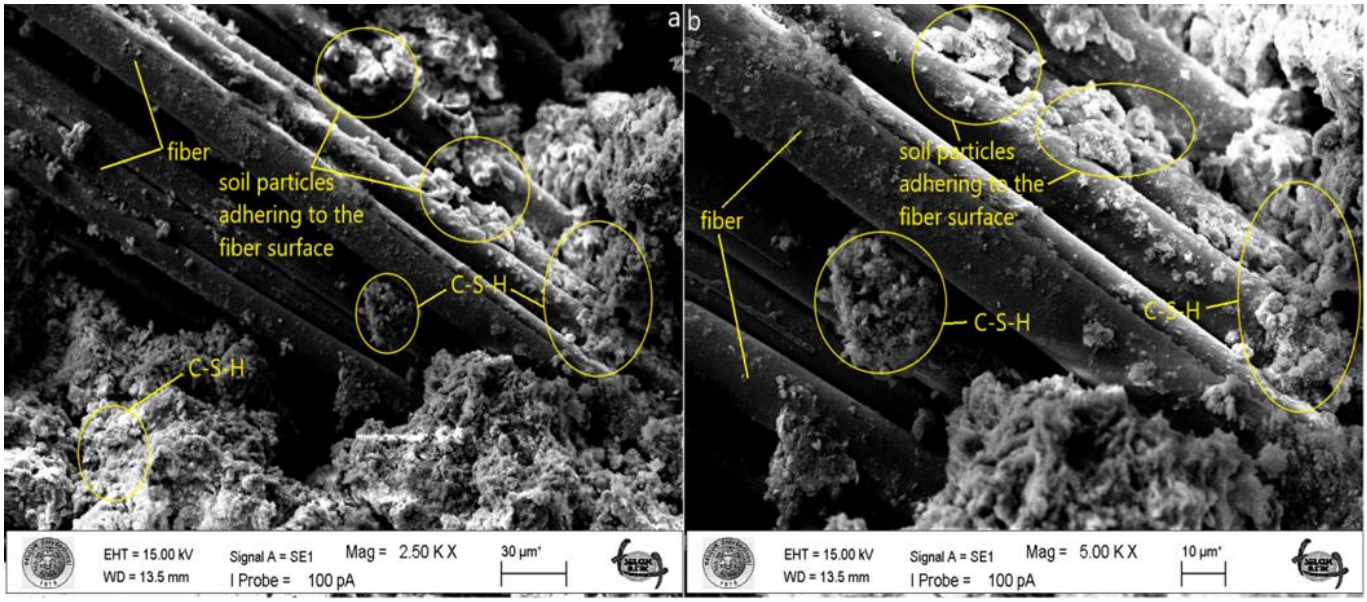

Figure 14. SEM image of design -10 (%3L+%0.5BF+%10SF additives) a. 2500X magnification; b. 5000X magnification.

In the area shown in Figure 14, it is observed that the basalt fiber surface, which is a good indicator of a strong bond between clay particles and basalt fibers, is held by many clay minerals. Due to the tightly reinforced interaction between basalt fibers and clay particles, they can collectively carry external loads, and the interfacial force between clay particles and basalt fibers gradually increases to resist the external load applied to the treated test specimens [28-29]. In this case, the surface roughness of the fiber plays an important role in improving the interfacial friction between the fiber and clay particles and enhances its resistance to external loading. Additionally, the main hydration products resulting from pozzolanic reactions (C-S-H gels) formed enhance the physical bonding strength among clay particles by cementing fine grains and filling pore voids. Hydration products also facilitate better adhesion of basalt fiber with the cementitious soil matrix.

When lime is added to clay, calcium ions react with clay minerals to form silicate gel. The filling effect of C-S-H also strengthens the bond between fiber and composite material, resulting in a more stable interfacial structure. Figure 14 clearly shows cementitious products on the fiber.

4. Conclusion

In this study, experimental studies were conducted to determine the effect of combinations of basalt fiber with fly ash and silica fume on the microstructure of a highly plastic clay. In order to increase the pozzolanic interaction, 3% lime was added to all mixtures in the experimental studies.

Based on SEM images, the untreated soil sample had a dispersed and porous structure as opposed to the treated combinations. Samples treated with just lime, lime combined with fly ash, and lime combined with silica fume showed a denser and more compact matrix structure, which was attributed to pozzolanic and cation exchange reactions. Particle surfaces were predominantly coated with hydration gels, which effectively filled soil pores. The images obtained supported the results of the strength tests.

SEM images revealed that soil particles adhered to the surface of the basalt fiber, enhancing the friction between the soil particles and the basalt fiber.

XRD analysis demonstrated the formation of calcium silica/alumina hydrate (C-S-H) minerals attributable to the pozzolanic reaction involving lime, fly ash, and silica fume additives. Moreover, the analysis results indicated the presence of quartz (SiO_2) in the samples. The density of quartz decreased due to the pozzolanic reaction induced by the additives.

The density of the calcium silicate/alumina hydrate mineral has been found to be higher in designs with high strengths. This situation indicates that during the curing period, the formation of hydrated gel occurs at higher concentrations with the use of optimum parameter levels for strength and an increase in curing time.

Author contributions

Atila Demiröz: Conceptualization, Methodology, Writing-Reviewing and Editing. **Onur Saran:** Laboratory Experiments, Writing-Original draft preparation, Software, Investigation.

Conflicts of interest

The authors declare no conflicts of interest.

References

1. Attom, M. F., Taqieddin, S. A., & Mubeideen, T. (2000). Shear strength and swelling stabilization of unsaturated clayey soil using pozzolanic material. Advances in Unsaturated Geotechnics, 275-288. https://doi.org/10.1061/40510(287)19

2. Ural, N. (2016). Effects of additives on the microstructure of clay. Road Materials and Pavement Design, 17(1), 104-119. https://doi.org/10.1080/14680629.2015.1064011
3. Indraratna, B., Vinod, J. S., & Athukorala, R. (2023). Chemically Treated Soils. DSC/HISS Modeling Applications for Problems in Mechanics, Geomechanics, and Structural Mechanics, 149-164.
4. Demiröz, A., Saran, O., & Hamed, E. A. A. (2023). The influence of various additives on the plasticity properties of clayey soil. Selcuk University Journal of Engineering Sciences, 22 (1), 38-42.
5. Mugambi, M. L. (2023). Evaluation of physico-chemical properties of expansive soils stabilized by limestone calcined clay cement. [Doctoral dissertation, Meru University of Science and Technology].
6. Al-Rawas, A. A., Hago, A. W., & Al-Sarmi, H. (2005). Effect of lime, cement and Sarooj (artificial pozzolan) on the swelling potential of an expansive soil from Oman. Building and Environment, 40(5), 681-687. https://doi.org/10.1016/j.buildenv.2004.08.028
7. Cuisinier, O., Auriol, J. C., Le Borgne, T., & Deneele, D. (2011). Microstructure and hydraulic conductivity of a compacted lime-treated soil. Engineering Geology, 123(3), 187-193. https://doi.org/10.1016/j.enggeo.2011.07.010
8. Davoudi, M. H., & Kabir, E. (2011). Interaction of lime and sodium chloride in a low plasticity fine grain soils. Journal of Applied Sciences, 11(2), 330-335. https://doi.org/10.3923/jas.2011.330.335
9. Jauberthie, R., Rendell, F., Rangeard, D., & Molez, L. (2010). Stabilisation of estuarine silt with lime and/or cement. Applied Clay Science, 50(3), 395-400. https://doi.org/10.1016/j.clay.2010.09.004
10. Prusinski, J. R., & Bhattacharja, S. (1999). Effectiveness of Portland cement and lime in stabilizing clay soils. Transportation Research Record, 1652(1), 215-227. https://doi.org/10.3141/1652-28
11. Bell, F. G. (1996). Lime stabilization of clay minerals and soils. Engineering Geology, 42(4), 223-237. https://doi.org/10.1016/0013-7952(96)00028-2
12. Chen, F. H. (2012). Foundations on expansive soils, 12. Elsevier.
13. Raj, P. P. (1999). Ground improvement techniques (HB). Firewall Media.
14. Metelková, Z., Boháč, J., Sedlářová, I., & Přikryl, R. (2011). Changes of pore size and of hydraulic conductivity by adding lime in compacting clay liners. Geotechnical Engineering: New Horizons, 93-98. https://doi.org/10.3233/978-1-60750-808-3-93
15. Muhmed, A., & Wanatowski, D. (2013). Effect of lime stabilisation on the strength and microstructure of clay. IOSR Journal of Mechanical and Civil Engineering, 6(3), 87-94.
16. Di Sante, M., Fratalocchi, E., Mazzieri, F., & Pasqualini, E. (2014). Time of reactions in a lime treated clayey soil and influence of curing conditions on its microstructure and behaviour. Applied Clay Science, 99, 100-109. https://doi.org/10.1016/j.clay.2014.06.018
17. Song, Y., Geng, Y., Dong, S., Ding, S., Xu, K., Yan, R., & Liu, F. (2023). Study on mechanical properties and microstructure of basalt fiber-modified red clay. Sustainability, 15(5), 4411. https://doi.org/10.3390/su15054411
18. Ma, Q. Y., Cao, Z. M., & Yuan, P. (2018). Experimental Research on Microstructure and Physical-Mechanical Properties of Expansive Soil Stabilized with Fly Ash, Sand, and Basalt Fiber. Advances in Materials Science and Engineering, 2018(1), 9125127. https://doi.org/10.1155/2018/9125127
19. ASTM D698 (2012). Standard test methods for laboratory compaction characteristics of soil using standard effort. West Conshohocken, USA, ASTM International.
20. Ayothiraman, R., & Singh, A. (2017). Improvement of soil properties by basalt fibre reinforcement. In Proc., DFI-PFSF Joint Conf. on Piled Foundations & Ground Improvement Technology for the Modern Building and Infrastructure Sector, 403-412.
21. Jia, Y., Zhang, J. S., Wang, X., Ding, Y., Chen, X. B., & Liu, T. (2022). Experimental study on mechanical properties of basalt fiber-reinforced silty clay. Journal of Central South University, 29(6), 1945-1956. https://doi.org/10.1007/s11771-022-5056-z
22. Taguchi, G. J. Q. R. (1987). Taguchi techniques for quality engineering. Quality Resources, New York.
23. Sharma, R. K., & Hymavathi, J. (2016). Effect of fly ash, construction demolition waste and lime on geotechnical characteristics of a clayey soil: a comparative study. Environmental Earth Sciences, 75, 1-11. https://doi.org/10.1007/s12665-015-4796-6
24. Türköz, M., Savaş, H., & Tasci, G. (2018). The effect of silica fume and lime on geotechnical properties of a clay soil showing both swelling and dispersive features. Arabian Journal of Geosciences, 11, 1-14. https://doi.org/10.1007/s12517-018-4045-x
25. Tiwari, N., Satyam, N., & Patva, J. (2020). Engineering characteristics and performance of polypropylene fibre and silica fume treated expansive soil subgrade. International Journal of Geosynthetics and Ground Engineering, 6(2), 18. https://doi.org/10.1007/s40891-020-00199-x
26. Wang, D., Abriak, N. E., & Zentar, R. (2013). Strength and deformation properties of Dunkirk marine sediments solidified with cement, lime and fly ash. Engineering Geology, 166, 90-99. https://doi.org/10.1016/j.enggeo.2013.09.007
27. Tang, C., Shi, B., Gao, W., Chen, F., & Cai, Y. (2007). Strength and mechanical behavior of short polypropylene fiber reinforced and cement stabilized clayey soil. Geotextiles and Geomembranes, 25(3), 194-202. https://doi.org/10.1016/j.geotexmem.2006.11.002
28. Ma, Q. Y., Cao, Z. M., & Yuan, P. (2018). Experimental Research on Microstructure and Physical-Mechanical Properties of Expansive Soil Stabilized with Fly Ash, Sand, and Basalt Fiber. Advances in Materials Science and Engineering, 2018(1), 9125127. https://doi.org/10.1155/2018/9125127
29. Wang, D., Wang, H., Larsson, S., Benzerzour, M., Maherzi, W., & Amar, M. (2020). Effect of basalt fiber

inclusion on the mechanical properties and microstructure of cement-solidified kaolinite. Construction and Building Materials, 241, 118085. https://doi.org/10.1016/j.conbuildmat.2020.118085